AD-A208 076

REPORT DOCUMENTATION PAGE

UNCLASSIFIED	1b. RESTRICTIVE MARKINGS
2a. SECURITY CLASSIFICATION AUTHORITY	3. DISTRIBUTION/AVAILABILITY OF REPORT
2b. DECLASSIFICATION/DOWNGRADING SCHEDULE	Approved for public release; distribution is unlimited.
4. PERFORMING ORGANIZATION REPORT NUMBER(S)	5. MONITORING ORGANIZATION REPORT NUMBER(S)
6a. NAME OF PERFORMING ORGANIZATION: Naval Ocean Systems Center	6b. OFFICE SYMBOL (If applicable): NOSC
6c. ADDRESS (City, State and ZIP Code): San Diego, CA 92152-5000	7a. NAME OF MONITORING ORGANIZATION
8a. NAME OF FUNDING/SPONSORING ORGANIZATION: Office of Naval Research	8b. OFFICE SYMBOL (If applicable): ONR
8c. ADDRESS (City, State and ZIP Code): 800 N. Quincy Street, Arlington, VA 22217	7b. ADDRESS (City, State and ZIP Code)
	9. PROCUREMENT INSTRUMENT IDENTIFICATION NUMBER

10. SOURCE OF FUNDING NUMBERS			
PROGRAM ELEMENT NO.	PROJECT NO.	TASK NO.	AGENCY ACCESSION NO.
0601153N	EE22	RR01103	DN307 332

11. TITLE (include Security Classification)

EFFECTS OF THE HUBBARD INTERACTION AND ELECTROSTATIC PINNING IN POLYACETYLENE

12. PERSONAL AUTHOR(S)

J. C. Hicks, J. T. Gammel

13a. TYPE OF REPORT	13b. TIME COVERED	14. DATE OF REPORT (Year, Month, Day)	15. PAGE COUNT
Professional paper	FROM TO	March 1989	

16. SUPPLEMENTARY NOTATION

17. COSATI CODES		
FIELD	GROUP	SUB-GROUP

18. SUBJECT TERMS (Continue on reverse if necessary and identify by block number)

polyacetylene, polythiophene, defect vibration, thiophenes, infrared spectroscopy, polymers, reprints, (again)

19. ABSTRACT (Continue on reverse if necessary and identify by block number)

The discrete model for the coupled electron-phonon system in polyacetylene has been extended to include the electronic effects of electrostatic pinning and the Hubbard interaction in the unrestricted Hartree-Fock approximation. To fit experimental structural data, the Hamiltonian also includes the lattice kinetic energy and the coupling of several vibrational degrees of freedom. This model is then used to self-consistently determine the electronic eigenstates and the structural configuration for an odd-membered ring. The electronic states from this equilibrium configuration are then used to calculate the charge and spin density, optical absorption, and the single-electron loop corrections to the dynamical matrix. The resulting vibrational modes are examined and used in conjunction with the self-consistent electronic states to calculate the infrared-absorption spectra. Assuming that the pinning arises from an oppositely charged soliton on an adjacent chain leads to a pinning frequency of ≤500 cm^{-1}, in excellent agreement with observed results. A value for the Hubbard interaction of 4 eV leads to an excellent fit for the rest of the infrared spectra and the optical absorption for both a charged and a neutral soliton.

Published in *Physical Review B*, Volume 37, Number 11, 15 April 1988-I.

20. DISTRIBUTION/AVAILABILITY OF ABSTRACT	21. ABSTRACT SECURITY CLASSIFICATION
[X] UNCLASSIFIED/UNLIMITED [ ] SAME AS RPT [ ] DTIC USERS	UNCLASSIFIED

22a. NAME OF RESPONSIBLE PERSON	22b. TELEPHONE (Include Area Code)	22c. OFFICE SYMBOL
J. C. Hicks	(619) 553-1588	Code 633

DD FORM 1473, 84 JAN — 83 APR EDITION MAY BE USED UNTIL EXHAUSTED. ALL OTHER EDITIONS ARE OBSOLETE.

UNCLASSIFIED
SECURITY CLASSIFICATION OF THIS PAGE

PHYSICAL REVIEW B VOLUME 37, NUMBER 11 15 APRIL 1988-I

Effects of the Hubbard interaction and electrostatic pinning in polyacetylene

J. C. Hicks and J. Tinka Gammel*
Materials Research Branch, Naval Ocean Systems Center, San Diego, California 92152-5000
(Received 15 June 1987; revised manuscript received 21 September 1987)

The discrete model for the coupled electron-phonon system in polyacetylene has been extended to include the electronic effects of electrostatic pinning and the Hubbard interaction in the unrestricted Hartree-Fock approximation. To fit experimental structural data, the Hamiltonian also includes the lattice kinetic energy and the coupling of several vibrational degrees of freedom. This model is then used to self-consistently determine the electronic eigenstates and the structural configuration for an odd-membered ring. The electronic states from this equilibrium configuration are then used to calculate the charge and spin density, optical absorption, and the single-electron loop corrections to the dynamical matrix. The resulting vibrational modes are examined and used in conjunction with the self-consistent electronic states to calculate the infrared-absorption spectra. Assuming that the pinning arises from an oppositely charged soliton on an adjacent chain leads to a pinning frequency of ≈ 500 cm^{-1}, in excellent agreement with observed results. A value for the Hubbard interaction of 4 eV leads to an excellent fit for the rest of the infrared spectra and the optical absorption for both a charged and a neutral soliton.

I. INTRODUCTION

The simple model of polyacetylene, $(CH)_x$, originally proposed by Su, Schrieffer, and Heeger[1] (SSH), has been very successful in explaining many experimental results. In order to develop a more quantitatively accurate model it is important to consider additional interactions outside the range of the original model. Thus in this study we propose to investigate the effects of both the Hubbard interaction and electrostatic pinning on the electronic and optical (visible and infrared) properties of polyacetylene in the presence of a soliton. The effects of pinning from a point charge on the optical absorption in $(CH)_x$ has been considered for a variety of configurations by Glick and Bryant.[2] The "minimum energy configuration" in that calculation was not obtained from a minimum energy self-consistency relation, nonetheless they obtained a rather nice fit with experimental results for the optical absorption of a charged soliton well removed from the end of the chain. In this work we consider the pinning resulting from a point charge, a reasonable point of view for some chemically doped samples, and in an effort to understand the finite "pinned" frequency for optically excited $(CH)_x$, the pinning resulting from an equal and oppositely charged soliton on an adjacent chain. (We have recently become aware of two independent studies using this same pinning concept, one using a phenomenological approach,[3] and another which calculates numerically the phonon eigenstates in the single component problem [4] to predict the frequency of the "pinned" mode in optically excited samples.)

The effects of the Hubbard interaction in the Hartree-Fock approximation on the electronic states in polyacetylene when localized defects are present have been considered with some success both numerically in the discrete model[5,6] and analytically in the continuum model.[7] With this in mind we have decided to incorporate the same approximation to calculate the electronic states in the discrete model for polyacetylene. We then extend these calculations to obtain the optical absorption for both charged and neutral solitons, the phonon modes for charged solitons, and the infrared absorption in polyacetylene. Recently the phonon modes with particular interest in the bound states have been studied in the presence of the Hubbard term[8] and a combination of the Hubbard term and pinning.[4] The effects of pinning and electron-electron repulsion appear to do a reasonable job of fitting the frequencies of the "pinned" mode for both chemically doped and optically excited samples.[4] However, since the vibrational modes in polyacetylene are more complex than those in a simple one dimensional single component model it is necessary to extend this model to one which includes three structural degrees of freedom. A very useful scheme, developed by Horovitz[9] (amplitude-mode or AM formalism) has been used with the framework of the continuum model[10] to study the spectrum of modes with large oscillator strengths associated with the translation of mobile defects, "T" modes. However it has been shown that additional ir active bound modes in the single component problem can result in additional satellite features (A^-) in the infrared spectra.[11,12] Thus the existence of the ir active third bound mode for a single structural degree of freedom in both the continuum model[13] and the discrete model[14-17] for polyacetylene should result in additional features in a realistic calculation of the infrared absorption. In fact these additional features have been predicted in a multicomponent calculation in the absence of pinning and Hubbard interactions in both the continuum model[18] and the discrete model with a semicontinuum approximation.[19] Calculating the phonon modes and the ir absorption in such a multiple component model enables one to not only fit the experimental frequencies and oscillator strengths,

of the three infrared active "T" modes which have relatively large large oscillator strengths but the frequencies and oscillator strengths of the satellite A^- localized modes as well. The prediction of these additional ir active modes has stimulated some recent experimental interest in the weak satellite (A^-) infrared absorption peaks.[20,21] The measured oscillator strengths for these A^- modes is smaller than that predicted by coupling the phonon modes to the electron-phonon induced current fluctuations in both the continuum model calculations[18] and the discrete model calculations.[19] We will show that with pinning and a value of 4 eV for the Hubbard interaction an excellent fit with infrared absorption data is obtained for both $(CH)_x$ and $(CD)_x$.

Additionally recent work by the authors has indicated that the width of the pinned mode may be an inherent property of polyacetylene due to strong mixing of the low frequency translational mode with low frequency acoustic phonons creating hybrid states in the acoustic phonon branch with large infrared oscillator strengths.[22] This would eliminate the need for a distribution of pinning potentials in the material. However, we show in this study that as the soliton becomes pinned this mixing is dramatically reduced and as originally postulated a distribution of pinning potentials or pinning parameters[9] is required to explain the experimentally observed width in the "pinned mode."

II. ELECTRONIC EIGENSTATES

To model polyacetylene we assume the Su, Schrieffer, and Heeger (SSH) Hamiltonian[1] with on site repulsion of the Hubbard type and screened Coulomb electrostatic pinning. The electrostatic pinning is only considered for charged systems and is modeled as either a point charge off the chain or as a distributed charge from an equal and opposite soliton residing on an adjacent chain. To model the vibrational modes we extend the SSH Hamiltonian to include multiple structural degrees of freedom in a matter analogous to that developed for the continuum model by Horovitz[9] (AM formalism). In all cases considered we initially calculate a self-consistent structural configuration and the corresponding eigenstates which depend strongly upon the electrostatic pinning and the strength of the Hubbard term. Since we are primarily concerned with the effects on the localized electronic state that occurs in this problem, we will consider the Hubbard term in the mean field unrestricted Hartree-Fock approximation when calculating the electronic eigenstates.

The SSH Hamiltonian with Coulombic pinning and on site Hubbard repulsion is given by

$$H=-\sum_{n,\sigma} t_{n,n+1}(c^{\dagger}_{n+1,\sigma}c_{n,\sigma}+c^{\dagger}_{n,\sigma}c_{n+1,\sigma})+\frac{K}{2}\sum_{n}(y_{n+1}-y_n)^2$$
$$+\frac{U}{2}\sum_{n,\sigma}(c^{\dagger}_{n,\sigma}c_{n,\sigma}-\tfrac{1}{2})(c^{\dagger}_{n,-\sigma}c_{n,-\sigma}-\tfrac{1}{2})+\sum_{n,\sigma}V(n)\,(c^{\dagger}_{n,\sigma}c_{n,\sigma}-\tfrac{1}{2}), \tag{2.1a}$$

with the hopping energy being proportional to the spacing between the carbon sites,

$$t_{n,n+1}=t_0-\gamma(y_{n+1}-y_n). \tag{2.1b}$$

The c's create and annihilate π electrons on the appropriate site and γ is the electron-phonon coupling constant. U is the Hubbard constant with $V(n)$ being the site dependent Coulomb pinning potential, and K represents the σ electron spring constant of the polyacetylene chain. In the unrestricted Hartree-Fock approximation the on site Hubbard repulsion is replaced with

$$U\sum_{n,\sigma}[\rho_{-\sigma}(n)-\tfrac{1}{2}](c^{\dagger}_{n,\sigma}c_{n,\sigma}-\tfrac{1}{2}). \tag{2.1c}$$

The quantity $\rho_{-\sigma}(n)-\frac{1}{2}$ is simply the excess charge with negative spin where $\rho_{-\sigma}$ is given by

$$\rho_{-\sigma}(n)=\sum_{k}{}' \psi^{*}_{k,-\sigma}(n)\psi_{k,-\sigma}(n), \tag{2.2}$$

and $\sum'_k$ is the sum only over occupied states. We choose $V(n)$ to be a screened electrostatic Coulomb potential in an anisotropic dielectric media of the form

$$V(n)=\frac{-\Gamma e^2}{\epsilon_2\sqrt{\epsilon_1}}\sum_{m,\sigma}\frac{[\rho_{\sigma}(m)-\tfrac{1}{2}]\exp(-\Lambda R_{n,m})}{R_{n,m}}, \tag{2.3a}$$

where

$$R^2_{n,m}=\frac{(n-m)^2a^2}{\epsilon_1}+\frac{d^2}{\epsilon_2}. \tag{2.3b}$$

For pinning in optically excited samples, we assume from x-ray diffraction data for polyacetylene[23] that a, the distance between carbon sites, is 1.23 Å and d, the interchain separation is 4.24 Å. Numerical values of the dielectric constant both parallel and perpendicular to the chain have been determined experimentally[24] to be $\epsilon_1=7.1$ and $\epsilon_2=1.8$. The integer m sums over the carbon sites on an adjacent chain and $\rho_{\sigma}(m)-\frac{1}{2}$ is taken to be the negative of the chain under consideration. Γ is a parameter that chosen to be 2 to take into account the reduced mass effect for a pair of solitons. Λ was chosen to fit the experimental data and found to be 0.59. For pinning in chemically doped systems the expression $\sum_{\sigma}[\rho_{\sigma}(m)-\frac{1}{2}]$ is replaced by a Kronecker delta function which centers a point charge at $m=(n+1)/2$, and Γ for this case is 1. Since polyacetylene is known to expand when it is doped,[25] the distance of the charged impurity from the chain is taken to be $0.52d$ rather than $0.5d$. In Sec. V, where we discuss the infrared activity of polyacetylene, it will be seen that this choice of parameters does an excellent job of fitting the frequencies of the "pinned" modes in polyacetylene.

The above Hamiltonian, Eq. (2.1), yields in the unrestricted Hartree-Fock approximation the following

difference equation for the electronic eigenstates,

$$E_{k,\sigma}\psi_{k,\sigma}(n)=t_{n-1,n}\psi_{k,\sigma}(n-1)+t_{n,n+1}\psi_{k,\sigma}(n+1)+\{U[\rho_{-\sigma}(n)-\tfrac{1}{2}]+V(n)\}\psi_{k,\sigma}(n). \quad (2.4)$$

Thus the eigenstates, $\psi_{k,\sigma}$, and eigenvalues, $E_{k,\sigma}$, are obtained by simply numerically diagonalizing this expression. To consider the problem of a chain with a single soliton, the total number of sites, N, is always chosen to be odd, and to avoid difficulties with end effects periodic boundary conditions are assumed. Taking a variational derivative of this Hamiltonian with respect to y_n leads to the self-consistency relation,

$$y_{n+1}-y_n=-\frac{\gamma}{K}\sum_{k,\sigma}{}'\,\psi^*_{k,\sigma}(n+1)\psi_{k,\sigma}(n)+\psi^*_{k,\sigma}(n)\psi_{k,\sigma}(n+1)+\text{const.} \quad (2.5)$$

To model polyacetylene we have chosen $2t_0=5$ eV, $4\gamma y_0/2t_0=\Delta_0/2t_0=0.14$ ($2\Delta_0$ being equal to the Peierls gap) which leads to a value of the dimensionless electron-phonon coupling constant of $\lambda=8\gamma^2/\pi K(2t_0)=0.4197$.

This self-consistency expression combined with Eq. (2.2) for both possible spins enables all of the input parameters to Eq. (2.3) to be determined from its own solutions. Thus Eq. (2.3) can be diagonalized repeatedly with new values of $y_{n+1}-y_n$ and $\rho_\sigma(n)$ calculated for each diagonalization until a minimum energy self-consistent solution is obtained within a specified convergence criteria. From the resulting electronic eigenstates it is straightforward to determine charge and spin densities for charged and neutral solitons as well as such parameters as the soliton excitation energy, gap state energy level, and the soliton width as a function of the Hubbard U. Quantitative values for these parameters can be very informative, for example the ratio of spin densities on even and odd sites (ρ_-/ρ_+) for a neutral soliton is strongly dependent on the strength of the Hubbard term. Electron-nuclear double-resonance (ENDOR) measurements have determined this ratio to be $-\frac{1}{3}$.[26] From our calculations this is consistent with $U\approx 3$--4 eV, which is consistent with earlier results.[5-7]

The full Hubbard term is given by

$$H_{\text{Hub}}=\frac{U}{2}\sum_{i,\sigma}(n_{i,\sigma}-\tfrac{1}{2})(n_{i,-\sigma}-\tfrac{1}{2}). \quad (2.6)$$

If we define $n_i=n_{i,\sigma}+n_{i,-\sigma}$ and the site dependent spin density $s_i=\frac{1}{2}(n_{i,\sigma}-n_{i,-\sigma})$, then we can rewrite the Hubbard term as

$$H_{\text{Hub}}=U\sum_i\left[\frac{(n_i-1)(n_i-1)}{4}-s_is_i\right]. \quad (2.7)$$

For a charged soliton s_i is zero, thus to minimize the energy the soliton width increases while for a neutral soliton n_i-1 is zero, and the effect of the Hubbard term is to decrease the soliton width. This is seen in our results where the relative soliton width increases from 1 to 1.18 for a charged soliton and decreases from 1 to 0.82 for a neutral soliton as U ranges from 0 to 4 eV. Again this is consistent with results of other investigators.[5-7] Also consistent with this interaction is a shift in the gap state energy. For a charged soliton we find that the gap state energy shifts from $E_{\text{gap}}=0$ for $U=0$ to $E_{\text{gap}}=\pm 0.134$ eV for $U=4$ eV with the $+$ sign corresponding to an n-type soliton and the $-$ sign corresponding to a p-type soliton. For a neutral soliton the energy shifts of the midgap state are more significant and the spin degeneracy is lifted. As U ranges from 0 to 4 eV the gap state for spin up (the occupied state) shifts from $E_{\text{gap}}=0$ to $E_{\text{gap}}=-0.396$ eV with the corresponding shift up for the spin down gap state. This will have some significance in the optical absorption, as we will see in the next section.

With the solutions to the self-consistent Hamiltonian described above, we are able to calculate many interesting properties of polyacetylene. In addition to the charge and spin density discussed above, we use these states to find the optical absorption, single electron loop corrections to the dynamical matrix and the corresponding vibrational states, and the infrared absorption spectra. Each of these calculations will be discussed in the following sections.

III. OPTICAL ABSORPTION

Since we are dealing with an extended system, it is awkward to deal directly with induced moments; consequently, we consider current-current correlations to calculate the conductivity, $\sigma(\omega)$. With the Hamiltonian of Eq. (2.1), the current density is expressed as

$$J(\tau)=i\sum_{n,\sigma}t_{n,n+1}(c^\dagger_{n+1,\sigma}c_{n,\sigma}-c^\dagger_{n,\sigma}c_{n+1,\sigma}). \quad (3.1)$$

In the Matsubara formalism the current-current correlation is given by

$$\pi(\tau)=-\langle T_\tau J(\tau)J(0)\rangle, \quad (3.2)$$

where T_τ is the imaginary time-temperature ordering operator. The retarded current-current correlation function is obtained by Fourier-series expanding in Matsubara frequencies and then analytically continuing $i\omega_n\rightarrow\omega+i\delta$. The frequency dependent conductivity is derived from this as

$$\sigma(\omega)=\text{Re}\frac{i\pi(\omega+i\delta)}{\omega}. \quad (3.3)$$

Following the usual formalism, where Wick's theorem is used to expand the current-current correlation function in terms of Green's functions and then using an eigenfunction expansion for these Green's functions, yields in the low-temperature limit

$$\sigma(\omega)=\frac{\pi}{\omega}\sum_{k,q,\sigma}{}''\,f_{k,q,\sigma}f_{q,k,\sigma}\,\delta(\omega+E_{k,\sigma}-E_{q,\sigma}), \quad (3.4a)$$

with

$$f_{k,q,\sigma}=\sum_i t_{i,i+1}[\psi_{k,\sigma}(i+1)\psi_{q,\sigma}(i)-\psi_{k,\sigma}(i)\psi_{q,\sigma}(i+1)], \quad (3.4b)$$

where $\sum''$ sums over empty k states and filled q states.

To be entirely consistent with our approximation of the effect of the Hubbard term on the optical absorption, we should include additional effects to the current-current correlation other than direct transitions between renormalized states. The result of such an effort would result in summing over a frequency dependent matrix element times the same joint density of states delta function. This would be only a small correction to optical conductivity and would significantly increase the difficulty of the calculation and hence is ignored.

The results of the calculations are somewhat dependent on the width of the Lorentzian used to represent the delta function in sum above. We typically use as small a value as possible and still have the absorption appear as a smooth curve. For a 101 site chain this requires the full width at half maximum (FWHM) to be $0.06(2t_0)$. The effect on the optical absorption of the Hubbard term for charged solitons is not surprising in that the main effect is simply a small shift in the midgap absorption band. However, as mentioned above the shift is more dramatic for a neutral soliton, and for the same Lorentzian half-width the inner-band transitions merge with interband transitions at about $U=4.0$ eV. In Fig. 1 we plot the optical absorption in a neutral soliton for both $U=3$ eV and $U=4$ eV. Since the experimentally observed optical absorption spectra are broader than those plotted in Fig. 1, we would expect from these calculations that the inner band transition could not be resolved experimentally for a value of U between 3 eV and 4 eV. Thus a value of U between 3 eV and 4 eV is again consistent with experimental observation, where very careful measurements of optical absorption in ammonia-compensated polyacetylene show no sign of inner band transitions.[27]

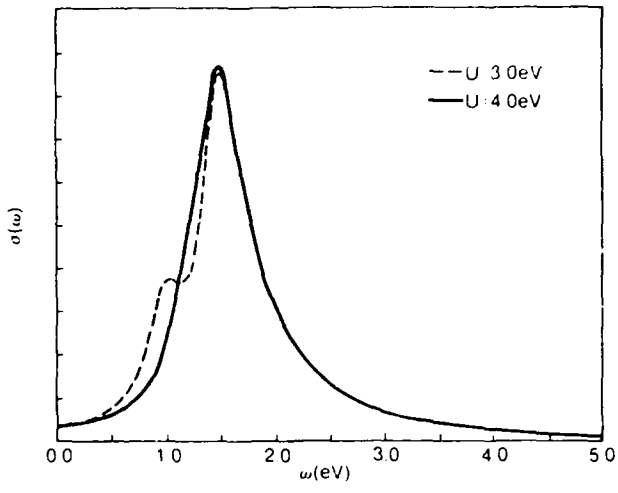

FIG. 1. Optical absorption for a neutral soliton with (dashed) $U=3.0$ eV and (solid) $U=4.0$ eV.

IV. VIBRATIONAL MODES

To make direct experimental comparison of structural vibrations we have chosen to extend the multicomponent concept of the AM formalism[9] to the discrete SSH model for polyacetylene. This model Hamiltonian includes the lattice kinetic energy and couples the π electrons to a set of displacement fields, $y_{\alpha,n}$, as well as the Hubbard and pinning terms,

$$H=-\sum_{n,\sigma} t_{n,n+1}(c^{\dagger}_{n+1,\sigma}c_{n,\sigma}+c^{\dagger}_{n,\sigma}c_{n+1,\sigma})+\tfrac{1}{2}\sum_{\alpha,n} K_{\alpha}(y_{\alpha,n+1}-y_{\alpha,n})^2+\tfrac{1}{2}\sum_{\alpha,n} M_{\alpha}\dot{y}_{\alpha,n}$$
$$+\frac{U}{2}\sum_{n,\sigma}(c^{\dagger}_{n,\sigma}c_{n,\sigma}-\tfrac{1}{2})(c^{\dagger}_{n,-\sigma}c_{n,-\sigma}-\tfrac{1}{2})+\sum_{n,\sigma} V(n)\,(c^{\dagger}_{n,\sigma}c_{n,\sigma}-\tfrac{1}{2}). \tag{4.1}$$

To maintain a fixed electronic gap, in analogy with the multicomponent continuum model, we take $\sum_{\alpha}\gamma_{\alpha}y_{\alpha,n}=\gamma y_n$, thus leaving $t_{n,n+1}$ unchanged. From self-consistency we find $(K_{\alpha}/\gamma_{\alpha})y_{\alpha,n}=(K/\gamma)y_n$, and defining a dimensionless electron phonon coupling for each component as $\lambda_{\alpha}=8\gamma_{\alpha}^2/\pi K_{\alpha}(2t_0)$ leads to $\sum_{\alpha}\lambda_{\alpha}=\lambda$.

In a system with strong electron-phonon coupling such as this, it is necessary to consider the screening induced by the electron-phonon interaction via charge fluctuations in the π electron gas. This is conveniently done using single electron loop perturbation theory depicted diagrammatically in Fig. 2(a). The adiabatic solution of the integral equation represented by this diagram in a mul-

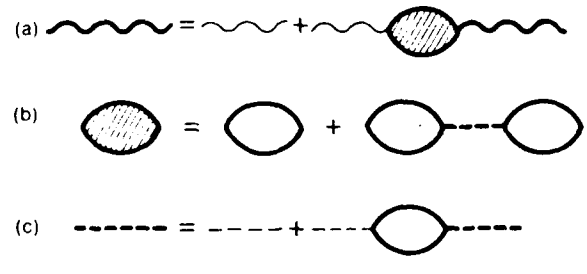

FIG. 2. The diagrammatic representations of (a) the integral equation for the vibrational modes, (b) electron-phonon induced charge fluctuations including all first order contributions from the Hubbard interaction, and (c) the integral equation for the screened Hubbard interaction.

ticomponent representation is equivalent to

$$\omega_{i,k}^2\phi_k(\alpha,n)=\frac{(\omega_\alpha^0)^2}{4}[2\phi_{i,k}(\alpha.n)-\phi_{i,k}(\alpha,n+1)-\phi_{i,k}(\alpha,n-1)]$$
$$+\pi\lambda\sum_{\beta,m}\left[\frac{\lambda_\alpha}{\lambda}\right]^{1/2}\omega_\alpha^0\,\Pi(n,m)\left[\frac{\lambda_\beta}{\lambda}\right]^{1/2}\omega_\beta^0\,\phi_{i,k}(\beta,m), \tag{4.2}$$

where $\Pi(n,m)$ is the electron-phonon induced polarization represented by the shaded bubble in Fig. 2(a). In this expression $(\omega_\alpha^0)^2$ is the bare $k=0$ optical phonon frequency squared and is given by $4K_\alpha/M_\alpha$, and the corresponding dimensionless coupling constant $\lambda_\alpha=8\gamma_\alpha^2/\pi K_\alpha(2t_0)$. These constants have been determined uniquely from Raman scattering data[28] and are listed in Table I for both $(CH)_x$ and $(CD)_x$. In a multicomponent description both the coupling constants, λ_α, and bare frequencies, ω_α^0, will be k dependent. However, the vibrational modes of interest are all near or at $k=0$ on either the acoustic or optical phonon branch. Since the electron-phonon interaction leaves the vibrational modes in the acoustic phonon branch virtually unchanged, and since the parameters are taken from a continuum model fit, which is appropriate for $k=0$ optical phonons, we assume that ignoring the k dependence of these constants will still result in physically meaningful results.

Since we are considering a many body term (Hubbard interaction), the outer electron lines in the polarization bubble are bold, indicating that they include the first order contribution of the Hubbard interaction to the proper self-energy. In a many body formalism this usually requires the solution of a Dyson equation; however, for this particular problem that is identical to the solution of the unrestricted Hartree-Fock problem as described in Sec. II. To be consistent with that level of approximation in our calculation of Π, we consider the additional contributions of the Hubbard interaction to the electron-phonon induced polarization shown in Fig. 2(b), where $\Pi=\Pi^{(1)}+\Pi^{(2)}$. As shown in Figs. 2(b) and 2(c), this additional contribution requires an infinite sum of bubble diagrams connected with the Hubbard constant U. Thus to solve the integral equation (4.2) above first requires summing all the contributions to the polarization. We perform this sum by first solving the integral equation that is represented diagrammatically in Fig. 2(c). If we define in the adiabatic approximation the bubble with two Hubbard vertices [Fig. 2(c)] as $\Pi^{(0)}(n,n')$, and the dressed Hubbard interaction as $V_{n,n'}$, then the integral equation in Fig. 2(c) is written as

$$V_{n,n'}=U\delta_{n,n'}+U\sum_m\Pi^{(0)}(n,m)V_{m,n'}, \tag{4.3a}$$

where

$$\Pi^{(0)}(n,n')=2\sum_{k,q}{}''\frac{\psi_k(n)\psi_q(n)\psi_k(n')\psi_q(n')}{E_k-E_q}. \tag{4.3b}$$

Since we intend to use these states to calculate the infrared absorption in polyacetylene, we are only interested in the phonon modes for a charged soliton. For the case of a charged soliton the electronic eigenstates are spin degenerate, thus we have dropped their spin dependence and included a factor of 2 in Eq. (4.3b). To solve this integral equation for $V_{n,n'}$, we start by simply diagonalizing $\Pi^{(0)}(n,n')$. $\Pi^{(0)}$ can then be expanded in terms of its orthonormal set of eigenfunctions as

$$\Pi^{(0)}(n,n')=\sum_k\mu_k\phi_k(n)\phi_k(n'). \tag{4.4}$$

In terms of these states the solution for $V_{n,n'}$ is simply

$$V_{n,n'}=U\sum_k\frac{\phi_k(n)\phi_k(n')}{1-U\mu_k}. \tag{4.5}$$

The second diagram in Fig. 2(b), which we define as $\Pi^{(2)}(n,n')$, although somewhat tedious, is now straightforward to evaluate. Keeping in mind that the outer vertices involve matrix elements of the electron-phonon interaction and that the internal vertices involve matrix elements of the Hubbard interaction, this diagram in the adiabatic approximation is expressed as

$$\Pi^{(2)}(n,n')=4\sum_{m,m'}\sum_{k,q}{}''\frac{g_{k,q}(n)\psi_k(m)\psi_q(m)}{E_k-E_q}V_{m,m'}\sum_{k',q'}{}''\frac{\psi_{k'}(m')\psi_{q'}(m')g_{k',q'}(n')}{E_{k'}-E_{q'}}, \tag{4.6}$$

where the electron-phonon vertex, $g_{k,q}(n)$, is given by

$$g_{k,q}(n)=\psi_k(n)[\psi_q(n+1)-\psi_q(n-1)]$$
$$+\psi_q(n)[\psi_k(n+1)-\psi_k(n-1)]. \tag{4.7}$$

Again with the factor of 4 we have taken advantage of the spin degeneracy of the electronic eigenstates. The expression for the first diagram on the right-hand side of

TABLE I. Coupling constants and bare optical phonon frequencies for $(CH)_x$ and $(CD)_x$.

	λ_α/λ		ω_α^0 (cm^{-1})	
α	$(CH)_x$	$(CD)_x$	$(CH)_x$	$(CD)_x$
1	0.07	0.06	1234	921
2	0.02	0.005	1304	1207
3	0.91	0.935	2040	2040

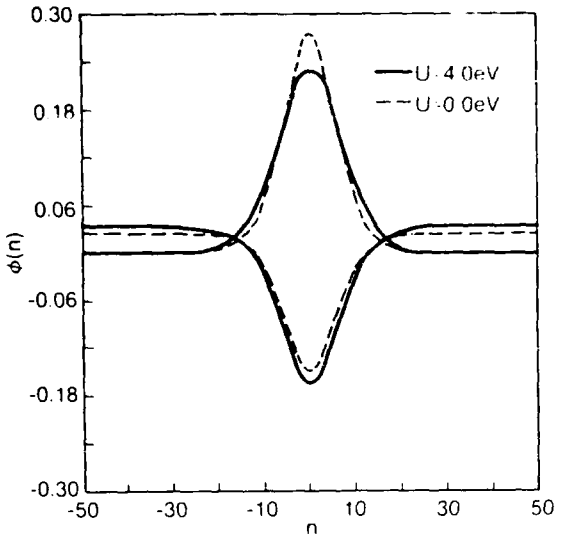

FIG. 3. The optical (upper curves) and acoustic (lower curves) components of the translation phonon mode for (dashed) $U=0$ eV and (solid) $U=4$ eV.

the equals sign in Fig. 2(b) is the usual one in the SSH model for adiabatic electron-phonon screening of the vibrational modes,

$$\Pi^{(1)}(n,m)=2\sum_{k,q}{}'' \frac{g_{k,q}(n)g_{q,k}(m)}{E_k-E_q}. \tag{4.8}$$

$\Pi^{(1)}$ and $\Pi^{(2)}$ are then summed and Eq. (4.2) is diagonalized to determine the phonon eigenstates of the multicomponent model.

As expected from continuum model results, this extension of the discrete model to include several structural degrees of freedom results in three ir active localized modes related to the translational mode of the soliton[9,11,12] and three additional ir active modes related to the third bound mode in the single component version of the SSH model.[14–17] In the absence of pinning the effects of the Hubbard term have relatively little effect on these bound modes. However, the coupling of the translational mode to the low frequency acoustic modes is enhanced as U increases from 0 eV to 4 eV. This is apparent in Fig. 3, where for simplicity we plot the acoustic and optical components of the translational mode for the single component model for both $U=0$ eV and $U=4$ eV. These results are physically reasonable, as the Hubbard term causes a local expansion of the lattice in the region of the soliton. The mixing for both cases is significantly larger than the original calculation,[22] which used a semicontinuum model[29] solutions for the electronic eigenstates. Thus if this mixing were maintained in the presence of pinning, it could explain the width of the pinned mode as an inherent property of the system.

The inclusion of pinning has a rather dramatic effect on the frequency of the translational mode as well as some smaller shifts in the higher frequency modes. With the choice of pinning parameters discussed and in the absence of the Hubbard term, the frequency of the pinned mode for an optically excited sample is shifted from near zero to 530 cm^{-1} and for a chemically doped sample to 805 cm^{-1} for $(CH)_x$. For $(CD)_x$ the corresponding frequency shifts are to 493 cm^{-1} and 778 cm^{-1}, respectively. These frequencies are somewhat high (low) for the optically excited (chemically doped) polyacetylene. However, when we include a Hubbard interaction with $U=4$ eV, these frequencies are shifted for both the optically and chemically doped systems. For $(CH)_x$ and $(CD)_x$ the pinned frequencies for optically excited samples become 503 cm^{-1} and 474 cm^{-1}, respectively, while for chemically doped systems the corresponding frequencies are 877 cm^{-1} and 767 cm^{-1}. These results are in excellent agreement with experimental results, implying that the mechanisms proposed in Sec. II for pinning are physically reasonable. However, at the pinned frequencies the wave number of the acoustic phonons is much larger than the inverse of the characteristic width of the phonons, thus the mixing of the translational mode with these states is dramatically reduced. This reduces the transfer of ir oscillator strength to the nearby acoustic modes, creating a relatively sharp ir active mode at the pinned frequency. Consequently, the experimentally observed width of the pinned mode is almost certainly due to a distribution in pinning potentials (or pinning parameters) in the polymer, and not the result of a distribution of oscillator strengths due to mixing with acoustic phonons.

V. INFRARED ABSORPTION

In Sec. III we discussed the optical absorption from the point of view of retarded current-current correlations. This bare contribution (with respect to the electron-phonon interaction) to the optical activity is represented by the single loop in Fig. 4(a) which contributes only the allowed electronic transitions to the optical conductivity. Turning on the lattice kinetic energy couples the ionic motions to the charge fluctuations of the π electron gas. This coupling transfers oscillator strength from the purely electronic transitions to lower frequency modes associated with the IR active vibrational modes. The relevant correction is expressed diagrammatically in Fig. 4(b),

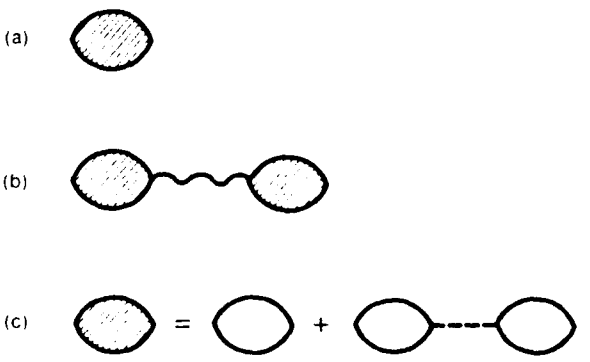

FIG. 4. The diagrammatic representations of (a) the current-current correlation, (b) correction to current-current correlation that includes low frequency ir active modes, and (c) current-current correlation including all first order contributions from the Hubbard interaction.

which makes a contribution to the current-current correlation function that oscillates at the frequency ω_{ik}. Consistent with our previous efforts in calculating the vibrational modes, we self-consistently consider the effects of the Hubbard term on the current fluctuations by summing all relevant bubble diagrams connected by the Hubbard term as shown in Fig. 4(c) and use the adiabatic approximation where appropriate.

The real part of the infrared conductivity for several lattice degrees of freedom is expressed as

$$\sigma(\omega)=\mathrm{Re}\left[\frac{i}{\omega}\sum_{m,m'} j(m,\omega+i\delta)\sum_{\alpha,\beta}\gamma_\alpha D_{\alpha,\beta}(m,m';\omega+i\delta)\,\gamma_\beta j(m',\omega+i\delta)\right], \tag{5.1}$$

where the Green's function, $D_{\alpha,\beta}$, representing the vibrational modes, is given by

$$D_{\alpha,\beta}(m,m';\omega+i\delta)=\frac{1}{\sqrt{M_\alpha M_\beta}}\sum_{i,k}\frac{\phi_{i,k}(\alpha,m)\phi_{i,k}(\beta,m')}{(\omega+i\delta)^2-\omega_{i,k}^2}. \tag{5.2}$$

The coupling between the vibrational modes and the electron gas is mediated by the electron-phonon interaction whose effects on the dynamical problem were discussed in the last section. The lowest order contribution (with respect to the Hubbard interaction) to the current fluctuations, $j^0(m,\omega+i\delta)$, is linear in ω and given by

$$j^0(m,\omega+i\delta)=\sum_{n,k,q}{}'' f_{k,q}g_{q,k}(m)\frac{2(\omega+i\delta)}{(\omega+i\delta)^2-(E_k-E_q)^2}, \tag{5.3}$$

where for the spin degenerate system being considered, $f_{k,q}$ is simply twice the original definition of $f_{k,q,\sigma}$. The higher order contributions to j are found with a technique exactly analogous to that described in Sec. IV. As an example we note that the expression representing the last diagram in Fig. 4(c) is nearly identical to Eq. (4.6); the only change is $f_{k,q}$ replacing the first $g_{k,q}(n)$. The effective coupling constant, γ_α/M_α, is more conveniently expressed in terms of the dimensionless coupling constant and the bare phonon frequency in the functional form $\sqrt{\lambda_\alpha}\omega_\alpha^0$. Since the vibrational frequencies are small compared to the electronic gap, the adiabatic approximation for this case is equivalent to ignoring only the frequency dependence in the denominator, and in general the expression for j is linear in ω and of the form $j(m,\omega)=2\omega K(m)$. The expression for the low frequency optical activity now reduces to

$$\sigma(\omega)=\frac{\pi^2}{4}\lambda(2t_0)\sum_{i,k}\left|\sum_{\alpha,n}\sqrt{\lambda_\alpha/\lambda}\,\omega_\alpha^0 K(n)\phi_{i,k}(\alpha,n)\right|^2 \times\delta(\omega-\omega_{i,k}). \tag{5.4}$$

Thus the contribution to the infrared conductivity is large only for vibrational eigenstates which overlap strongly with the electron-phonon induced current fluctuations. In general these fluctuations are localized at the defect site and thus only localized states with the correct symmetry can exhibit any oscillator strength.

We perform the dot product in Eq. (5.4) numerically for a variety of Hubbard interaction strengths for both unpinned, and optically and chemically pinned solitons. The results for both $(CH)_x$ and $(CD)_x$ are very enlightening. In Fig. 5 we present the results for unpinned $(CH)_x$ with both $U=0$ eV and $U=4$ eV. The most noticeable change is the increased width of the low frequency absorption due to mixing with the acoustic phonons. Another significant difference is the increase in relative oscillator strength in the satellite A^- modes. However for $U=0$ eV the oscillator strengths in these modes are substantially larger than that observed experimentally and of even more significance is that the center of the pinned mode, depending on the pinning mechanism, exists at either ≈ 500 cm^{-1} or ≈ 850 cm^{-1}. To better approximate this experimental data and hopefully under-

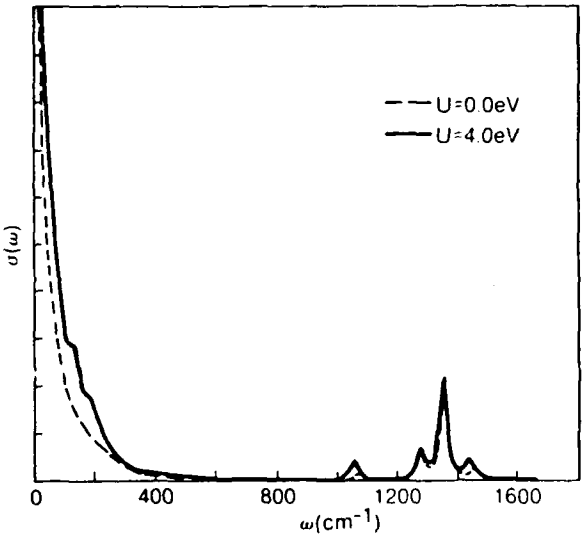

FIG. 5. The infrared absorption in $(CH)_x$ with no pinning and a Hubbard term of (dashed) $U=0$ eV and (solid) $U=4$ eV.

stand the source of the pinning, in Figs. 7(a) and 7(b) we plot the results for pinning due to an equal and opposite soliton on an adjacent chain for both $U=0$ eV and $U=4$ eV. Other than the shift of the pinned mode to a finite frequency, ≈ 530 cm^{-1}, the satellite peaks have virtually disappeared for $U=0$ eV. Thus pinning depletes the oscillator strength of the A^- modes while increasing the oscillator strength of the modes related to the uniform translational mode of the soliton. In view of recent studies, we know that the Hubbard interaction deepens the effective well for the bound state vibrational modes.[8] The electrostatic pinning is of the opposite sign of the Hubbard term, making it reasonable that the bound state phonons related to the third bound mode of the single component problem become more extended and carry less oscillator strength (OS). Additionally the transfer of OS to the translation type modes is consistent with the AM formalism[9] which transfers ir activity to these modes as the pinning parameter is increased. It is interesting, however, that a value $U=4$ eV restores a significant amount of ir activity to the A^- modes, and the solid curve in Fig. 6(b) does an excellent job of fitting the experimental data for optically excited $(CH)_x$,[21,30] which is displayed as an inset in this same figure.[30] Note the signature of the A^{-1}, in both the experimental and theoretical results, as a shoulder on the dominant absorption peak at 1360 cm^{-1}. When including pinning and a U of 4 eV, we obtain frequencies of 503 cm^{-1}, 1280 cm^{-1}, and 1360 cm^{-1} for the translational modes. Their relative oscillator strengths (OS) are 44, 1.0, and 5.0 respectively, which compare quite favorably with measured values.[21] The satellite peaks now occur at 1074 cm^{-1} and 1456 cm^{-1} with OS of 0.11 and 0.15. For completeness and for comparison with experimental data, Fig. 7 shows the results of the infrared absorption for chemically doped $(CH)_x$ with $U=4$ eV, where the predicted pinned frequency is 877 cm^{-1} with an OS of 54. The additional two translational-type modes occur at 1283 cm^{-1} and 1389 cm^{-1} with relative oscillator strengths of 1.0 and 14.8. At first glance it appears the OS of the mode at 1283 cm^{-1} is inconsistent with the mechanism of transferring oscillator strengths to these modes as the pinning is increased. This can be easily explained; one of the A^- modes occurs at 1280 cm^{-1} and experimentally cannot be resolved from the mode at 1283 cm.$^{-1}$ Since pinning reduces the OS of the A^- modes, the net effect is a slight reduction of the OS of this peak. In Fig. 8, we plot the results for $(CD)_x$ with the Hubbard constant $U=4.0$ eV for both optically and chemically generated solitons. For optically excited samples the pinned mode occurs at 474 cm^{-1}. The additional strongly ir active translational modes for optically excited solitons occur at 1042 and 1215 cm^{-1}. These modes have OS of 32.4, 9.8, and 1.0, respectively, which again are in relatively good agreement with experimental data.[21] For these conditions the only observable satellite peak occurs at 1358 cm^{-1} with an OS of 0.15. For chemically doped $(CD)_x$ we predict that the pinned frequency occurs at 766 cm^{-1} and the two additional translational modes at 1138 cm^{-1} and 1233 cm^{-1}. These modes have relative oscillator strengths of 2.0, 2.1, and 1.0, respectively. Again our results predict only one observable satellite peak, which occurs at 1402 cm^{-1} with an OS of 0.03.

The experimental observation[21] of the satellite feature in $(CH)_x$ at ≈ 1050 cm^{-1} is somewhat questionable due

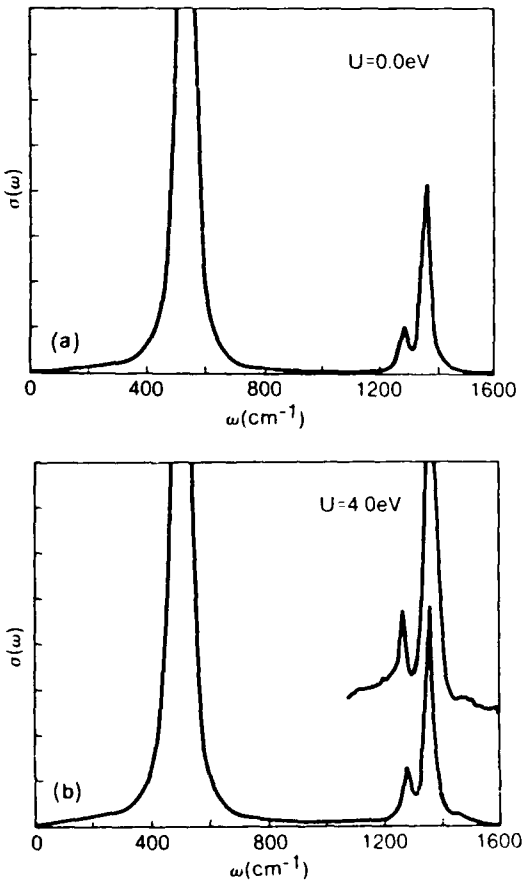

FIG. 6. The infrared absorption in $(CH)_x$ with optically induced pinning for (a) $U=0$ eV and (b) $U=4$ eV; the inset here shows experimental data for the frequency range 1200 cm^{-1} to 2000 cm^{-1}.

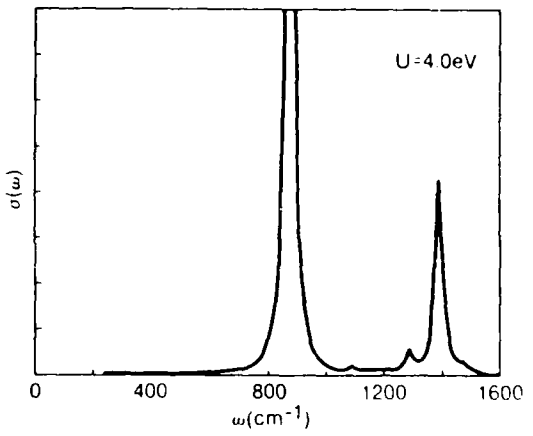

FIG. 7. The infrared absorption in $(CH)_x$ with chemically induced pinning for $U=4$ eV.

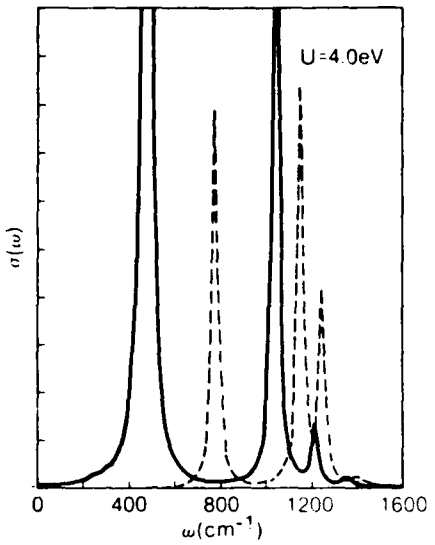

FIG. 8. The infrared absorption in $(CD)_x$ with (dashed) optically and (solid) chemically induced pinning for $U=4$ eV.

to the existence of a large naturally occurring ir mode at approximately the same frequency and the corresponding difficulty of accurately subtracting this large peak. However, the peak at approximately 1440 cm^{-1} has no such problem and is a clear marker for A^- vibrational modes in $(CH)_x$. Since pinning is required to fit the pinned mode in this material, then as we have seen that the OS of this satellite feature at 1441 cm^{-1} can be used to qualitatively fit the strength of the Hubbard interaction in $(CH)_x$. Consistent with the results of fitting the spin density and optical absorption for a neutral soliton, we find that a good fit is obtained with $U \approx 4$ eV. These secondary features in $(CD)_x$ also show a reasonable fit for the same value of U.

VI. CONCLUSION

In this study we have considered the effects of pinning and the Hubbard interaction on various electronic and optical properties, as well as an extension of the discrete SSH model to include several degrees of freedom. Several conclusions are possible from fits with experimental data. First, for optically excited samples our postulated mechanism for pinning, an equal and oppositely charged soliton on an adjacent chain, does an excellent job of fitting the frequency of the pinned mode in these materials. As one would expect for chemically doped samples, a point charge off the chain does a good job of creating a potential well with the correct pinning frequency, providing that the distance from the chain is increased to account for some expansion upon doping.[25] We have also demonstrated that the width of the experimentally observed pinned mode is probably not an inherent property of the system due to a transfer of oscillator strengths to modes in the acoustic phonon branch. It appears that a distribution of pinning potentials (or pinning parameters) is necessary to explain this width.

Probably the most interesting result of this study is the number of experiments: spin density distribution from ENDOR measurements,[26] optical absorption for a neutral soliton,[27] and the infrared oscillator strengths of the satellite A^- modes[21]— that can all be explained by including an effective Hubbard term with $U \approx 3-4$ eV. The consistency of all of these results validates the use of the unrestricted Hartree-Fock approximation of the Hubbard term when considering effects of electron-electron repulsion for a chain where the electronic and optical properties are dominated by the localized gap state that occurs in this system.

Comparisons of experimental data to the theoretical SSH model yields excellent agreement when we additionally include (i) electrostatic pinning for charged solitons, (ii) the Hubbard term, and (iii) several structural degrees of freedom.

ACKNOWLEDGMENTS

The authors are grateful to H. E. Schaffer and A. J. Heeger for communication of preliminary results. J. T. G. was supported by the Office of Naval Technology. J. C. H. was supported by the Office of Naval Research under Contract No. N001487WR24253.

*Permanent address: Los Alamos National Laboratory (Mail Stop B262), University of California, Los Alamos, NM 85745.

[1]W. P. Su, J. R. Schrieffer, and A. J. Heeger, Phys. Rev. Lett. **42**, 1698 (1979), and Phys. Rev. B **22**, 2099 (1980); **28**, 1138(E) (1982).
[2]Arnold J. Glick and Garnett W. Bryant, Phys. Rev. B **34**, 943 (1986).
[3]W. P. Su, Phys. Rev. B **36**, 6040 (1987).
[4]Richard J. Cohen and Arnold J. Glick, Phys. Rev. B **36**, 2907 (1987).
[5]K. R. Subbaswamy and M. Grabowski, Phys. Rev. B **24**, 2168 (1981).
[6]S. Kivelson and D. E. Heim, Phys. Rev. B **26**, 4278 (1982).
[7]Wei-Kang Wu and Steven Kivelson, Phys. Rev B **33**, 8546 (1986).
[8]C. Wu and X. Sun, Phys. Rev. B **33**, 8772 (1986).
[9]B. Horovitz, Solid State Commun. **41**, 729 (1982).
[10]H. Takayama, Y. R. Lin-Liu, and K. Maki, Phys. Rev. B **21**, 2388 (1980).
[11]E. J. Mele and J. C. Hicks, Phys. Rev. B **32**, 2703 (1985).
[12]J. C. Hicks and E. J. Mele, Phys. Rev. B **34**, 1091 (1986).
[13]H. Ito, A. Terai, Y. Ono, and Y. Wada, J. Phys. Soc. Jpn. **53**, 3520 (1984).
[14]A. Terai and Y. Ono, J. Phys. Soc. Jpn. **55**, 213 (1986).
[15]X. Sun, C. Wu, and S. C. Chen, Solid State Commun. **56**, 1039 (1985).
[16]K. A. Chao and Y. Wang, Phys. Scr. **34**, 177 (1986).
[17]J. Tinka Gammel and J. C. Hicks, Synth. Met. **17**, 63 (1987).

[18]Y. Ono, A. Terai, and Y. Wada, J. Phys. Soc. Jpn. **55**, 1656 (1986).

[19]J. C. Hicks and J. Tinka Gammel, Synth. Met. **17**, 57 (1987).

[20]Z. Vardeny, E. Ehrenfreund, O. Brafman, B. Horovitz, H. Fujimoto, J. Tanaka, and M. Tanaka, Phys. Rev. Lett. **57**, 2995 (1986).

[21]H. E. Schaffer, R. H. Friend, and A. J. Hegger, Phys. Rev. B **36**, 7537 (1987).

[22]J. C. Hicks and J. Tinka Gammel, Phys. Rev. Lett. **57**, 1320 (1986).

[23]C. R. Fincher, Jr., C. E. Chen, A. J. Heeger, and A. G. MacDiarmid, Phys. Rev. Lett. **48**, 100 (1982).

[24]H. Kahlert and G. Leising, Mol. Cryst. Liq. Cryst. **117**, 1 (1985).

[25]J. C. W. Chien, *Polyacetylene: Chemistry, Physics, and Material Science* (Academic, New York, 1984).

[26]A. J. Heeger and J. R. Schrieffer, Solid State Commun. **48**, 207 (1983); H. Thomann, L. R. Dalton, M. Grabowski, and T. C. Clarke, Phys. Rev. B **31**, 3141 (1985).

[27]B. R. Weinberger, C. B. Roxlo, S. Etemad, G. L. Baker, and J. Orenstein, Phys. Rev. Lett. **53**, 86 (1984).

[28]B. Horovitz, Z. Vardeny, E. Ehrenfreund, and O. Brafman, Synth. Met. **9**, 215 (1984).

[29]J. Tinka Gammel, Phys. Rev. B **33**, 5974 (1986).

[30]30. T. E. Jones, J. W. Schindler, P. A. Moser-Boss, C. S. Bendall, C. A. Smith, J. C. Hicks, and L. A. Lambert (unpublished)